Circadian variation in renal blood flow and kidney function in healthy volunteers monitored using non-invasive magnetic resonance imaging

PER ECKERBOM[1], PETER HANSELL[2], ELEANOR COX[3], CHARLOTTE BUCHANAN[3], JAN WEIS[4], FREDRIK PALM[2], SUSAN FRANCIS[3] & PER LISS[1]

[1]Section of Radiology, Department of Surgical Sciences, University Hospital, Uppsala, Sweden

[2]Department of Medical Cell Biology, Uppsala University, Uppsala, Sweden

[3]Sir Peter Mansfield Imaging Centre, University of Nottingham, Nottingham, UK

[4]Department of Medical Physics, University Hospital, Uppsala, Sweden

Short title: Circadian rhythm in renal perfusion and function

Correspondence:

Per Eckerbom, MD

Department of Radiology

University Hospital

751 85 Uppsala, Sweden.

E-mail: per.eckerbom@akademiska.se

Phone: +46186110000

Abstract

Circadian regulation of kidney function is involved in maintaining whole-body homeostasis and dysfunctional circadian rhythm can potentially be involved in disease development. Magnetic Resonance Imaging (MRI) provides reliable and reproducible repetitive estimates of kidney function non-invasively without the risk of adverse events associated with contrast agents and ionizing radiation. The purpose of this study was to estimate circadian variations in kidney function in healthy human subjects using MRI, and relate the findings with urinary excretions of electrolytes and markers of kidney function.

Phase Contrast imaging, Arterial Spin Labeling and Blood Oxygen Level Dependent R_2^*-mapping were used to assess the total renal blood flow and regional perfusion, and intrarenal oxygenation in eight female and eight male healthy volunteers every fourth hour during a 24h period. Parallel with MRI scans, standard urinary and plasma parameters were quantified.

Significant circadian variations of total renal blood flow were found over 24h with increasing flow from noon to midnight and decreasing flow during the night. In contrast, no circadian variation in intrarenal oxygenation was detected. Urinary excretions of electrolytes, osmotically active particles, creatinine and urea all displayed circadian variations, peaking during the afternoon and evening hours.

In conclusion, total renal blood flow and kidney function, as estimated from excretion of electrolytes and waste products, display profound circadian variations, whereas intrarenal oxygenation displays significantly less circadian variation.

Key words: Circadian variation, Kidney function, Magnetic Resonance Imaging, Arterial Spin Labeling, BOLD, Healthy volunteers.

Introduction

Many processes in humans and animals, including sleep-wake patterns, cardiac output, blood pressure and also numerous renal functions are influenced by circadian rhythm (1). Knowledge of daily fluctuations in biological processes was gained early with the first studies published in 1861 (2, 3). Recent years have seen a growing interest in this field with a steadily increasing number of published studies and in 2017 the Nobel prize in Physiology or Medicine was awarded for the discovery of specific circadian clock genes. This growing interest has, at least in part been driven by the finding that disruption of circadian patterns is associated with disease (4, 5). The main pacemaker of the circadian clock is located in the suprachiasmatic nucleus of the brain (6). Suprachiasmatic nucleus is controlled by light signals transmitted from the retina through the retinohypothalamic tract and is synchronized with the light/dark cycle. The signal substance melatonin is synthesized in the pineal gland and released into the blood circulation in a circadian rhythm controlled by the suprachiasmatic nucleus (7). The rise in melatonin at night has been shown to affect a number of biological processes, to promote sleep and to decrease body temperature (8, 9). It has been demonstrated in animal models that melatonin alters blood flow to assorted vascular beds by the activation of different melatonin receptors (10, 11). Cook *et al.* demonstrated that melatonin also affects renal blood flow in humans (12). Moreover, circadian alterations in glomerular filtration (GFR), tubular reabsorption and tubular secretion have been described (5, 13). Mills and Stanbury reported circadian alterations for urine flow and urinary excretions of Na^+ and K^+ (14). A number of different renal mechanisms influenced by a circadian rhythm and genetics were highlighted by Solocinski *et al.* in a review from 2015 (15). There are studies demonstrating daily variations of rat kidney oxygenation as measured using implanted oxygen electrodes (16, 17). To our knowledge, no previous work has studied circadian aspects of intrarenal perfusion and oxygenation in humans. Our research group and others have previously shown that non-invasive magnetic resonance imaging (MRI)

provides reliable and reproducible biomarkers of kidney function (18-20). In this study, we use phase contrast imaging, Arterial Spin Labeling (ASL) and Blood Oxygen Level Dependent (BOLD) R_2^*-mapping to assess total renal blood flow and regional perfusion, and intrarenal regional oxygenation to test the hypothesis that renal blood flow, perfusion and oxygenation display circadian variations.

Materials and Methods

Subjects

The Institutional Review Board of Uppsala University, Sweden, approved all protocols and informed consent was obtained from each subject before inclusion in the study. Eight female and eight male healthy non-smoking volunteers took part in this study (Table 1). To assure normal renal anatomy, all subjects were scanned with ultrasound prior to the study. The volunteers were instructed to avoid excessive physical exercise, alcohol, coffee and tea 12h prior to the start of the study. The study was performed during four study occasions with four participating subjects on each day. The volunteers arrived fasted at 7 am for blood sampling and to receive a urine catheter for continuous urine collection. MRI scans of the first, second, third and fourth subject commenced at around 8, 9, 10, and 11 am, respectively, hence, the study was divided into 6 measurement periods, 08:01-12:00, 12:01-16:00, 16:01-20:00, 20:01-24:00, 00:01-04:00, and 04:01-08:00. Urine parameters were also followed with a period of 4 hours. All participants were given three standardized meals including water during the study. Breakfast was served between 08:00-09.00, lunch between 12:00-13:00 and dinner between 17:00-18:00. The subjects were at rest in during the whole examination period and in supine position during the night.

Data acquisition

Subjects were scanned on a 3T MR scanner (Philips, Achieva, Best, The Netherlands). A 16-channel torso phased array coil together with a spine coil served for signal reception. Subjects were positioned supine. Breath-hold balanced turbo field echo images were acquired in axial, sagittal and coronal directions to guide subsequent imaging planning for the study. A respiratory triggered T_2-weighted (T_2w) turbo spin echo sequence was used for anatomical imaging (echo time (TE) 80 ms, field of view (FOV) 368x259 mm^2, acquisition matrix

244x247, 11 contiguous slices, slice thickness 5.5 mm, bandwidth/pixel 664 Hz). These images were also used for kidney volume assessment. Phase contrast MRI was acquired to measure renal artery blood flow using a single slice ECG triggered turbo field echo (TFE) sequence (TR/TE 7.8/3.6 ms, FOV 280x144 mm^2, matrix 240x140, bandwidth/pixel 382 Hz). Fifteen measures of blood flow in the renal arteries were collected across the cardiac cycle during a single breath hold (15-20 sec) bilaterally. Regional renal perfusion was quantified using a flow sensitive alternating inversion recovery (FAIR) ASL sequence (21). The selective inversion slice and a non-selective slab thickness were 25 mm and 400 mm, respectively. A single inversion time of 1300 ms was used to allow blood to traverse the vasculature and perfuse the kidney. Thirty-two control/label images were collected. To generate a kidney T_1 map, three sets of images were acquired at each of the 300, 400, 600, 800, 1000, 1200, 1400 and 1600 ms inversion times using a respiratory-triggered T_1-mapping scheme with non-selective slab thickness of 400 mm (18). The respiratory-triggered ASL and T_1-mapping utilized a balanced fast field echo readout scheme (TR/TE 3/1.5 ms, FOV 288x288 mm^2, acquisition matrix 96x96 mm^2, bandwidth/pixel 1085 Hz, spatial resolution 2x2x5 mm^3). with all measurements triggered to be collected at the end of expiration. A multiecho fast field echo (mFFE) sequence was used to quantify the blood oxygenation level dependent (BOLD) relaxation rate (R_2* = 1/T2*) (TR 84 ms, FOV 288x288 mm^2, initial TE 5 ms, echo spacing 3 ms, 12 echoes, matrix 192x192, bandwidth/pixel 620 Hz, single breath hold ~17 s) with a matched spatial resolution of 2x2x5 mm^3. Three multislice fast field echo measurements were collected during three breath holds. The total measurement time of the entire session was approximately 40-45 minutes.

Measurement of urinary parameters

Urine flows were measured gravimetrically, urinary Na+ and K+ concentrations were determined by flame spectrophotometry (model IL543, Instrumentation Lab, Milan, Italy) and

urine osmolality was determined by freezing point technique (Model 210, The Fiske Micro-Sample Osmometer Advanced Instruments, MA, USA). Urinary protein concentration was determined using DC Protein Assay (Bio-Rad Laboratories, Hercules, CA, USA). Creatinine in urine was determined colorimetrically using LabAssayTM Creatinine (Wako Pure Chemical Industries, Zurich, Switzerland). Thiobarbituric acid reactive substances (TBARS) were analyzed as previously described (22). Briefly, samples were mixed with thiobarbituric acid and heated to 97°C for 60 minutes followed by cooling and mixing with methanol containing 1 mM NaOH. Samples were mixed and centrifuged before supernatant was analyzed for florescence using excitation/emission of 532/553 nm. The concentration was derived using a standard curve of malondialdehyde.

Urinary excretion rates was calculated by multiplying urine concentrations with urine flow.

Data processing

Mean cross-sectional area of the lumen (mm^2), mean renal artery flow velocity (cm/s), and hence mean renal artery blood flow (ml/s) over a cardiac cycle was computed using the Q-flow software package (Philips Healthcare). Regional renal perfusion and T_1 maps were computed using software (MATLAB, The Mathworks Inc., Natick, MA, USA). to model the calculation of rRBF calculation as described by Kwong *et al.* (23) and Francis *et al.* (24). R_2^* was quantified by the Philips Research Integrated Development Environment (PRIDE) software package. A single Region of Interest (ROI) encompassing most of the cortical parenchyma was chosen for the analysis of renal cortex (Fig. 1B). Mean regional renal perfusion and R_2* values were evaluated for both kidneys in the cortex, outer and inner medulla. The outer and inner medulla was defined as the outer and inner half of the medulla. Mean values of quantified measures in the medulla (inner and outer) were calculated from four different ROI positions (Fig. 1B). These ROIs were adjusted in size and positioned based on the T_2w TSE anatomical image avoiding

any large vessels. ImageJ (NIH, Bethesda, MD, USA) software was used for ROI analysis of regional maps. Manual segmentation of the T_2w TSE images was used to calculate total kidney volume (TKV). Kidney weight was calculated assuming a kidney tissue density of 1.0 g/cm^3 and thereafter global renal perfusion was computed as a ratio of total renal blood flow measured from PC-MRI to kidney weight. The Mosteller formula was used to calculate body surface area (m^2) = body weight (kg) x height (m)/3600$^{1/2}$ (25).

Statistics

MRI data were tested for normality and are presented as mean±SD. The unpaired Student's t-test was used to compare MRI data between gender. Multiple comparisons across time were performed using an ANOVA followed by Fishers PLSD test. Correlations were evaluated by linear regression (GraphPad Software Inc, La Jolla, CA, USA).

The analysis of urinary data was divided into six 4h periods (8:01-12:00, 12:01-16:00, 16:01-20:00, 20:01-24:00, 00:01-04:00 and 04:01-08:00). Mean values were calculated for each subject and in each period. Since multiple measurements per subject were available, the data were evaluated using a mixed model approach (26) as implemented in the Mixed procedure of the SAS software (SAS Institute Inc, Cary, NC, USA). Subject and the subject vs. time interaction were regarded as random factors, while time was used as a fixed factor. Post-hoc pairwise comparisons were adjusted for multiplicity using Tukey's method. $P<0.05$ was considered statistically significant.

Results

Table 1 summarizes the characteristics of the study subjects. Representative examples of T_2-weighted, regional renal blood flow, and R_2* images are shown in Fig. 1A together with typical placement of ROIs in Fig. 1B. Mean regional renal perfusion and R_2* values in cortex, outer and inner medulla over the 24h period for all, female and male study subjects are shown in

Table 2. No significant difference in regional renal perfusion was found neither between the right and left kidneys nor between the genders. For R_2*, no significant difference was found between the right and left kidneys but for outer medulla a significant difference was found between the genders with slightly higher values in males. Total renal blood flow was quantified using PC-MRI in all 16 subjects. Double renal arteries (one right sided, and two left sided) were found in three male subjects. In these cases, total renal blood flow was computed by the summation of the blood flow through both renal arteries (19). Total renal blood flow was significantly different (P=0.05) between genders, 829±149 ml/min and 1168±212 ml/min for females and males respectively (average right and left kidney, mean over 24h), but not between the right and left kidneys.

Significant variations of total renal blood flow were found during the course of the 24h both in females and males (Fig. 2). Total renal blood flow was increased during the late afternoon/evening hours (16:01-20:00) and (20:01-24:00) compared to the early afternoon and night. Average cortical, outer and inner medullary regional renal perfusion was 311±44, 84±6, and 34±4 ml/min/100 g, respectively (mean over 24h, all subjects). No significant variations in cortical, outer or inner medullary regional renal perfusion were found over the period of 24h in neither all, female nor male subjects, this is shown summed across right and left kidney in Fig. 3, however, cortical regional renal perfusion shows a similar pattern of diurnal changes to that of total renal blood flow (Fig. 2). Mean renal volume was 173±31 ml (female: 151±20 and male: 194±25 ml). No statistical difference in total kidney volume was found between the right and left kidneys for a given subject, though a significant difference was found in total kidney volume between genders (P<0.01). A strong correlation was found between total renal blood flow and body surface area (P<0.01) when looking at all subjects though this correlation for females and males separately did not reach significance (Fig 4). Also, a significant correlation was found between total renal blood flow and total kidney volume (P<0.001) for all subjects

and males but not for females (Fig. 5). Global perfusion as measured from TKV corrected PC-MRI total renal blood flow showed significant circadian fluctuations when looking at all subjects but not for females and males independently (Fig. 6). No significant difference regarding global perfusion was found between the genders. Average cortical, outer and inner medullary R_2* was 16.5±0.8, 25.4±0.8 and 34.1±1.7 s^{-1} (mean over 24h, all subjects). No significant variations in cortical, outer or inner medulla R_2* were found over the 24h period neither for all, female nor male study subjects (Fig. 7).

Mean values of urine biomarkers are shown in Table 3. Urine flow reveals significant circadian variations with highest values during the afternoon and values dropping during the night hours (Fig. 8A). Creatinine clearance demonstrates significant circadian variations with maximum values during the evening hours and values dropping during the night (Fig. 8B). Urine urea excretion shows a significant difference between the genders with a significant circadian pattern with rising values during the day and evening hours and lower values during the night and early morning for all and male subjects but not for female subjects (Fig. 9). Na^+ excretion also show significant differences between the genders and exhibits significant circadian variations with maximum values during the evening hours and lower values during the day and night for all and male subjects but not for female subjects. (Fig. 10). For tubular Na^+ excretion, significant circadian changes were seen with values dropping during the night hours (Fig. 11A). Fractional Na^+ excretion gradually increased during the day and evening and dropped during the night (Fig. 11B). K^+ excretion showed a significant circadian rhythm with highest values during the day and lower values during the morning and evening/night hours (Table 4). Urine osmolality excretion reveals a significant circadian pattern with highest values during the evening hours and lower values during the morning and night (Table 4). For urine TBARS excretion, no significant circadian variation was found (Table 4). Average urine protein excretion showed no significant circadian variation (Table 4). Urine creatinine excretion demonstrated significant

circadian variations with maximum values during the evening hours and values dropping during the night (Table 4).

Discussion

In this study we demonstrate circadian variations in total renal blood flow and global renal perfusion in healthy volunteers using completely non-invasive high-resolution magnetic resonance imaging. Total renal blood flow was collected in this study using PC-MRI and regional blood flow using ASL with a FAIR labelling scheme. Dynamic contrast enhanced MRI techniques can also be used to assess regional blood flow, but due to the invasive nature of these methods they cannot be used to assess repeated measures over a 24-hour period. Renal ASL measures have previously been validated against gold standard methods of para-aminohippurate clearance, microspheres, ultrasound, and scintigraphy. Our results using PC MRI and ASL are concordant with previous findings (19, 27, 28). Further the use of a FAIR scheme is in-line with the renal consensus paper, however here we use a bFFE readout rather than a single-slice spin-echo EPI readout as this provides higher spatial resolution to select ROIs in the cortex, outer and inner medulla. Although previous studies have reported circadian variations in several physiological parameters in the mammalians (1, 7), this is, to the best of our knowledge, the first indication of circadian variations associated with renal blood flow and perfusion in humans.

Regulation of renal blood flow and glomerular filtration is multifactorial (29), involving both neuronal and hormonal control of renal perfusion pressure, vascular tone and tubular handling of electrolytes. The sympathetic innervation varies during the day and decreases during sleep (30). Cardiac output and arterial blood pressure, controlled in part by sympathetic activity, fluctuates with activity level during the day and decreases at night (31, 32), potentially reducing renal perfusion. The well-known night time decrease in blood pressure is commonly referred to as “nocturnal dipping”. Notably, lack of nocturnal dipping is strongly associated with increased cardiovascular risk (33-35). In the kidney, sympathetic activity modulates renin release from granular cell located in the distal part of the afferent arterioles, vascular tone of

renal resistance vessels and transepithelial tubular Na^+ transport (36). Renin release is the rate limiting step controlling the angiotensin II signaling, which influences vascular tone and extracellular volume via angiotensin II AT_1-receptor activation (37). Due to the direct effects on renal perfusion pressure and vascular regulation, sympathetic signaling is also directly involved in regulation of GFR (38). The effect of sympathetic signaling on tubular Na^+ transport is mediated via both direct neuronal signaling and via secondary effects of angiotensin II signaling to affect tubular transporter activity, location and expression levels (39). The renin angiotensin system has been found to be strongly influenced by the sleep/awake cycle (40, 41) with markedly elevated levels of renin during sleep, regardless of when sleep occurs (42). Still, a diurnal variation in the renin angiotensin system, independent of posture and diet has been reported in previous studies (43, 44).

Vasopressin is a neuropeptide synthesized primarily in the brain that promotes the reabsorption of water in the kidneys (45). Besides that, vasopressin is also an important regulator of circadian rhythm in the suprachiasmatic nucleus (46, 47), controlled by the light cycle (48, 49). It may be speculated that circadian variation in vasopressin levels protects against dehydration during the inactive phase of the 24h day cycle when water intake is limited (45).

Melatonin is another hormone that exhibits significant diurnal variations closely related to the circadian fluctuations of sympathetic innervation, renin and aldosterone (40, 50, 51) and it has been shown that kidney impairment is associated with alteration in the endogenous melatonin rhythm (52). It has also been shown that melatonin can ameliorate chronic kidney disease by suppressing the renal renin-angiotensin system (51).

In this study, we found a significant decrease in renal blood flow, Na^+ excretion and urine flow during sleep, which is consistent with the increased nocturne levels of renin reported in previous studies (40, 41). However, given the detected significant circadian fluctuations in total renal blood flow, no significant circadian variation in regional renal perfusion were detected in the

present study. For renal cortex perfusion there was a similar pattern as for total renal blood flow, although this did not reach statistical significance. It can be seen that the curve for cortical regional blood flow (perfusion) resembles that for total renal blood flow, but the change in cortical perfusion did not reach statistical significance over time. It should be noticed that regional perfusion is computed from voxel-wise fit to the ASL perfusion curve and this will have a lower signal change since the regional changes reflects the blood flow per voxel (and also involves an individual voxel fit) compared to the total flow through the vessel measured using PC-MRI for total blood flow. The lack of medullary regional blood flow variation likely relates to the relative insensitivity of the detection technique at these even lower perfusion rates.

Na^+ balance and volume homeostasis are absolutely vital for human life and largely depend on normal kidney function (53). In this study, Na^+ excretion revealed significant circadian variations, peeking during the evening hours with lower Na^+ excretions during the day and night. Similar circadian variations have previously been shown in human as well as in animal studies (14, 54, 55). Decreased Na^+ excretion could either be due to decreased tubular Na^+ load due to decreased glomerular filtration or by increased tubular Na^+ reabsorption. Interestingly, increased angiotensin II signaling, secondary to increased renin release, would increase Na^+ reabsorption similarly to the observed low urinary Na^+ excretion during night hours.

Urine production, also under intricate hormonal control (56), has previously been shown circadian variations (14, 57), which is more profound in younger subjects (58, 59). Our results are in line with these findings showing decreased urine flow during the inactive night hours.

The kidneys are extremely well-perfused receiving approximately 20-25% of cardiac output (60), but extracting only 10-20% of the delivered oxygen (61). All of the blood entering the kidney reaches kidney cortex, but only about 10% is perfusing the renal medulla, resulting in relative hypoxia in this part of the kidney (62) (63, 64). Interestingly, the renal medulla is extremely sensitive to ischemic injury, which is attributed to the high energy demand by the

medullary thick ascending limb of the loop of Henle in the relation to the relatively low oxygen delivery to this region (63).

About 80% of total kidney oxygen consumption is attributed to active tubular electrolyte transport (65). Therefore, it could be reasonable to assume that renal tissue oxygenation would fluctuate with alterations in Na^+ reabsorption. Indeed, Emans *et al.* reported profound circadian fluctuations in renal oxygenation with increased intrarenal oxygen levels during dark hours in rats (16). However, we could not detect any circadian variation in intrarenal oxygenation, as determined by renal R_2*, in healthy humans in any region of the kidney. The significant difference between females and males found for outer medullary oxygenation is probably due to the relatively low number of subjects in each group. Several mechanisms have been proposed to protect kidney oxygen homeostasis (66), (67), and intrarenal hypoxia is an acknowledged unifying pathway to chronic kidney disease (68). However, it should also be acknowledged that renal R_2* not only reflects blood oxygenation but is also sensitive to changes in the intrarenal blood volume fraction, the oxy-Hb dissociation curve, and haematocrit, as well as non-physiological measures such as magnetic field inhomogeneities (e.g. due to poor shimming or air interfaces) which can also influence the measured R_2* value. In future we will explore the use of recently validated renal TRUST (T2 -relaxation-under-spin-tagging (TRUST) MRI for assessment of renal oxygen delivery and absolute O2 consumption, but this was not available at the time of this scan.

Creatinine clearance and urinary urea excretion dropped during the night, which is in good agreement with earlier reports (69), and has been attributed to the rise in vasopressin levels during the night. Glomerular filtration is a complex process (70), involving regulation of capillary hydrostatic pressure, permeability of the filtration barrier and tubular hydraulic resistance mainly attributed to volume reabsorption of downstream tubular segments. Furthermore, the integrity of the filtration barrier, as estimated by urinary leakage of proteins,

is one of the best predictors of progression of chronic kidney disease. In the healthy subjects included in the present study, urinary protein excretion was border lining detection limit and did not display any circadian variation although previous studies have reported a correlation between circadian variations in GFR and urinary protein excretion (71, 72).

Also, the circadian variation in urinary K^+ excretion in the present study is in good agreement with previous knowledge (14, 73).

Urinary excretion of TBARS, indicative of oxidative stress status, did not fluctuate during the 24h. TBARS is commonly used to estimate oxidative stress levels in pathological conditions such as diabetes (74) and hypertension (75). Possibly, urinary TBARS excretion may not have enough sensitivity to detect normal variations when levels are low.

The nature of the imaging technique used in the present study inflicts some limitations that potentially could influence the results. The study subject had to be placed in the scanner every fourth hour, which meant they had to be woken during the normally inactive night hours, however they sat upright performing everyday tasks (such as reading and using a computer), but avoiding exercise, during the daytime hours. However, the results from the present study are in good agreement with previously those reported results, implying that this study design did not significantly impact on the outcome. Also we did not collect blood pressure measures at each time point, rather this was measured only in the morning, just prior to the first MRI scan.

In conclusion, total renal blood flow and kidney function display distinct significant circadian variations, whereas intrarenal oxygenation seems to display significantly less circadian variation. This may indicate that tight control of intrarenal oxygen homeostasis is of great importance for long-term kidney function.

Acknowledgements

This study was supported by the Swedish Research Council for Medicine and Health, the Swedish Diabetes Foundation, the Swedish Children Diabetes Foundation, the Ernfors Family Foundation, the Selanders Foundation, the Olga Jönsson Foundation, Region Uppsala and ALF funding from Uppsala University hospital. This work was also supported by a Royal Society International Exchange Programme Award.

Table 1. Characteristics of the study population.

	Total (N=16)	Female (N=8)	Male (N=8)
Age (y)	23±4	24±5	23±2
Body weight (kg)	69±11	63±8	76±11*
Height (cm)	176±10	169±4	184±9**
Body mass index (kg/m^2)	22.4±1.7	22.0±1,9	22.5±1.6
Body surface area (m^2)	1.84±0.20	1.71±0.12	1.97±0.19**
Heart rate (bpm)	66±10	69±8	63±11
Systolic blood pressure (mmHg)	121±11	114±7	127±12*
Diastolic blood pressure (mmHg)	74±7	72±7	76±6
Plasma Na^+ (mmol/l)	140±1	140±1	141±1
Plasma K^+ (mmol/l)	3.7±0.2	3.7±0.2	3.8±0.2
Plasma creatinine (μmol/l)	80±18	68±13	92±15**
Plasma urea (mmol/l)	4.5±1.2	4.2±1.0	4.8±1.3
Plasma glucose (mmol/l)	5.4±0.6	5.1±0.5	5.8±0.6*
Serum C-peptide (mmol/l)	0.62±0.16	0.64±0.20	0.60±0.13
$HbA1_c$ (mmol/mol)	34±1	34±1	34±1

Data presented as mean±SD. * denotes P<0.05 vs female, and ** demotes P<0.01 vs female.

Table 2. Mean regional renal blood flow (rRBF) and mean regional renal oxygenation (rRenal oxygenation) in the cortex, outer and inner medulla for all, female and male study subjects over the 24h period.

	Cortex (N=16)	Outer medulla (N=16)	Inner medulla (N=16)
rRBF (ml/100g/min) All	311±58	84±9*	34±7*§
rRBF (ml/100g/min) Female	322±57	82±9*	33±7*§
rRBF (ml/100g/min) Male	301±59	86±9*	36±7*§
rRenal oxygenation (R_2*; s^{-1}) All	16.5±0.8	25.4±0.8*	34.1±1.6*§
rRenal oxygenation (R_2*; s^{-1}) Female	16.3±0.6	25.0±0.6*	33.6±1.4*§
rRenal oxygenation (R_2*; s^{-1}) Male	16.7±0.9	25.9±0.7*ϒ	34.5±1.8*§

Data presented as mean±SD. * denotes P<0.001 vs cortex, § demotes P<0.001 vs outer medulla and ϒ denotes P<0.01 vs female.

Table 3. Urinary excretions of electrolytes, osmotically active particles, TBARS, protein, creatinine and urea in all study subjects.

	All subjects (N=16)	Female (N=8)	Male (N=8)
Urine flow (ml/min)	1.6±0.9	1.6±1.0	1.6±0.8
Urinary Na^+ excretion (mmol/min)	0.14±0.07	0.14±0.07	0.15±0.07*
Urinary K^+ excretion (mmol/min)	0.07±0.03	0.06±0.02	0.07±0.03
Urinary osmolar excretion (mOsm/min)	0.73±0.23	0.64±0.23	0.82±0.20*
Urinary TBARS excretion (nmol/min)	0.02±0.07	0.04±0.09	0.00±0.00
Urinary protein excretion (mg/min)	0.01±0.02	0.01±0.02	0.00±0.00
Urinary creatinine excretion (µmol/min)	8.5±3.3	6.9±3.0	10.3±2.6**
Urinary urea excretion (mmol/min)	0.40±0.20	0.32±0.21	0.48±0.15*

Data presented as mean±SD. * denotes P<0.05 vs female, and ** denotes P<0.01 vs female.

Table 4. Circadian variations of urinary excretions of K^+, osmotically active particles, TBARS, protein and creatinine in all study subjects (N=16 in all groups).

Time of day	08:01-12:00	12:01-16:00	16:01-20:00	20:01-24:00	00:01-04:00	04:01-08:00
Urianry K^+ excretion (mmol/min)	$0.07\pm0.01^{\mu\nu\gamma}$	$0.11\pm0.01^{\chi\beta\nu\gamma}$	$0.09\pm0.01^{\rho\nu\gamma}$	$0.07\pm0.01^{\theta\tau\gamma}$	$0.03\pm0.01^{\chi\mu\sigma\rho}$	$0.03\pm0.01^{\chi\mu\sigma\beta}$
Urinary osmolar excretion (mOsm/min)	$0.70\pm0.06^{\rho}$	$0.79\pm0.06^{\Psi}$	$0.80\pm0.06^{\Psi}$	$0.85\pm0.06^{\phi\gamma}$	$0.72\pm0.06^{\varepsilon}$	$0.62\pm0.06^{\phi\pi\beta}$
Urinary TBARS excretion (nmol/min)	0.01±0.01	0.01±0.01	0.02±0.01	0.02±0.01	0.01±0.01	0.01±0.01
Urinary protein excretion (mg/min)	0.01±0.00	0.01±0.00	0.01±0.00	0.01±0.00	0.00±0.00	0.00±0.00
Urinary creatinine excretion (µmol/min)	8.50±0.85	8.86±0.85	9.43±0.85	$9.64\pm0.84^{\phi}$	7.30±0.87	7.33±0.88

Data presented as mean±SD. $^{\varepsilon}$ denotes P<0.05 vs 20:01-24:00, $^{\phi}$ denotes P<0.05 vs 00:01-04:00, $^{\gamma}$ denotes P<0.05 vs 04:01-08:00, $^{\pi}$ denotes P<0.01 vs 12:01-16:00, $^{\theta}$ denotes P<0.01 vs 16:01-20:00, $^{\rho}$ denotes P<0.01 vs 20:01-24:00, $^{\tau}$ denotes P<0.01 vs 00:01-04:00, $^{\Psi}$ denotes P<0.01 vs 04:01-08:00, $^{\chi}$ denotes P<0.001 vs 08:01-12:00, $^{\mu}$ denotes P<0.001 vs 12:01-16:00, $^{\sigma}$ denotes P<0.001 vs 16:01-20:00, $^{\beta}$ denotes P<0.001 vs 20:01-24:00, $^{\nu}$ denotes P<0.001 vs 00:01-04:00, and $^{\gamma}$ denotes P<0.001 vs 04:01-08:00.

Figure legends

Figure 1. A: Representative T_2-weighted (anatomical information), regional renal perfusion (arterial spin labeling; ASL) and transverse relaxation rate (R2*; blood oxygen level dependent; BOLD) oxygenation images. B: Typical positioning of the regional of interest in cortex (red), outer (yellow) and inner medulla (green).

Figure 2. Circadian variation in total renal blood flow, data shown for mean and SD of all (A), female (B) and male (C) study subjects.

Figure 3. Circadian variation in regional renal perfusion in cortex, outer medulla and inner summed across right and left kidney, data shown for mean and SD of all (A), female (B) and male (C) study subjects.

Figure 4. Correlations between total renal blood flow and body surface area for all (A), female (B) and male (C) study subjects.

Figure 5. Correlations between total renal blood flow and total renal volume for all (A), female (B) and male (C) study subjects.

Figure 6. Circadian variation in global renal perfusion shown for mean and SD of for all (A), female (B) and male (C) study subjects.

Figure 7. Circadian variation in regional renal oxygenation in cortex, outer medulla and inner medulla, time points shown the mean and SD across all (A), female (B) and male (C) study subjects.
all study subjects.

Figure 8. Circadian variation in urine flow (A) amd creatinine clearance (B), time points show the mean and SD across all study subjects..

Figure 9. Circadian variation in urinary excretion of Urea. Time points shown the mean and SD across all (A), female (B) and male (C) study subjects.

Figure 10. Circadian variation in urinary excretion of Na^+. Time points shown the mean and SD across all (A), female (B) and male (C) study subjects.

Figure 11. Circadian variation in tubular Na^+ transport (A) and fractional Na^+ excretion (B), time points shown the mean and SD across all study subjects.

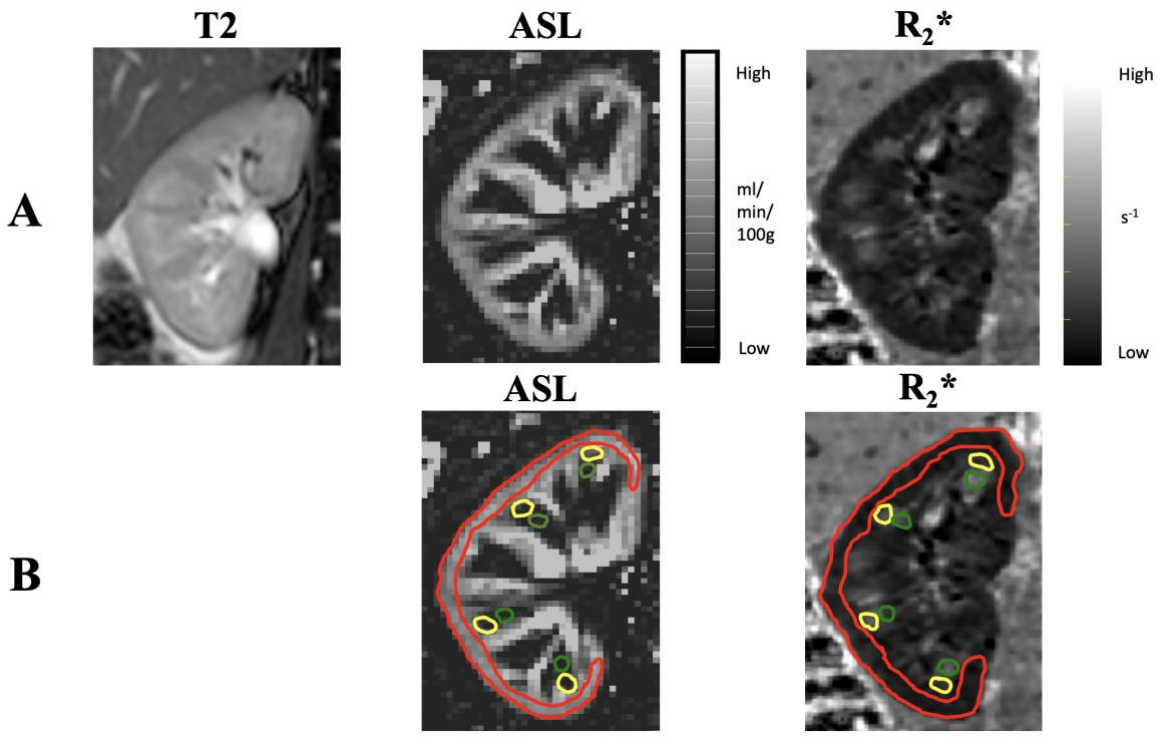

Figure 1.

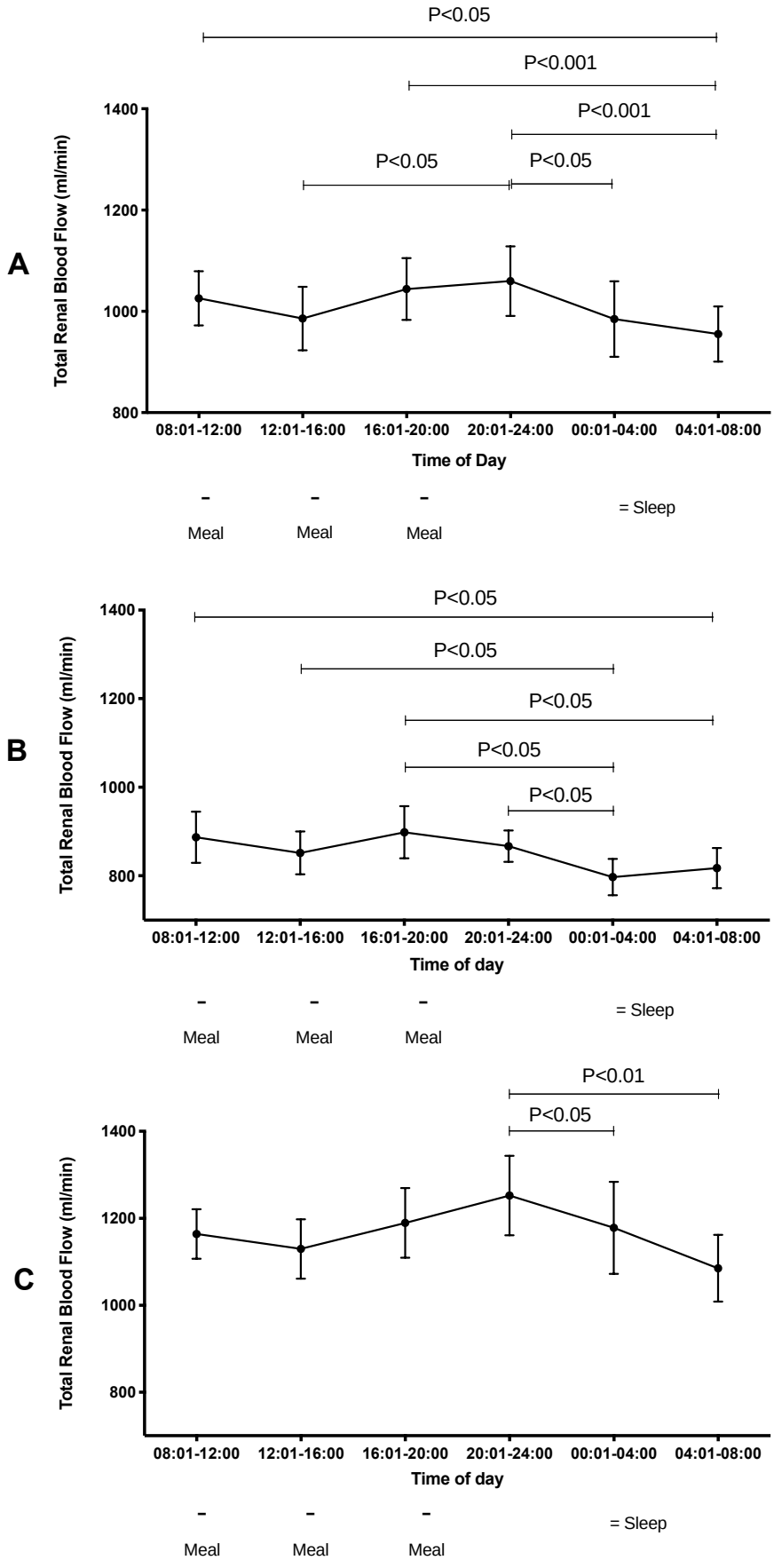
A
P<0.05
P<0.001
P<0.001
P<0.05
P<0.05
Total Renal Blood Flow (ml/min)
1400
1200
1000
800
08:01-12:00
12:01-16:00
16:01-20:00
20:01-24:00
00:01-04:00
04:01-08:00
Time of Day
Meal
Meal
Meal
= Sleep
B
P<0.05
P<0.05
P<0.05
P<0.05
P<0.05
Total Renal Blood Flow (ml/min)
1400
1200
1000
800
08:01-12:00
12:01-16:00
16:01-20:00
20:01-24:00
00:01-04:00
04:01-08:00
Time of day
Meal
Meal
Meal
= Sleep
C
P<0.01
P<0.05
Total Renal Blood Flow (ml/min)
1400
1200
1000
800
08:01-12:00
12:01-16:00
16:01-20:00
20:01-24:00
00:01-04:00
04:01-08:00
Time of day
Meal
Meal
Meal
= Sleep

Figure 2.

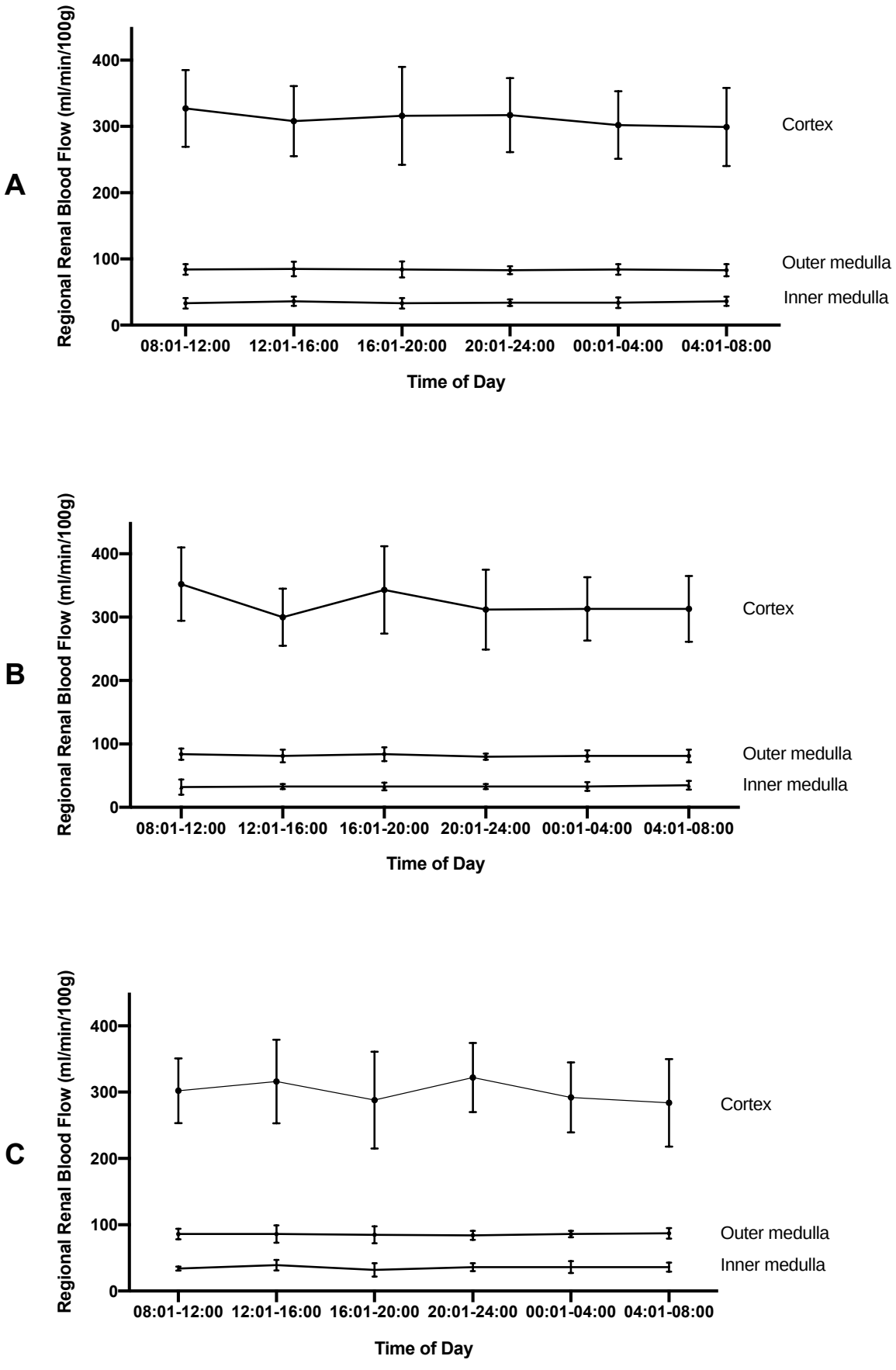
A
B
C
Regional Renal Blood Flow (ml/min/100g)
400
300
200
100
0
08:01-12:00
12:01-16:00
16:01-20:00
20:01-24:00
00:01-04:00
04:01-08:00
Time of Day
Cortex
Outer medulla
Inner medulla

Figure 3.

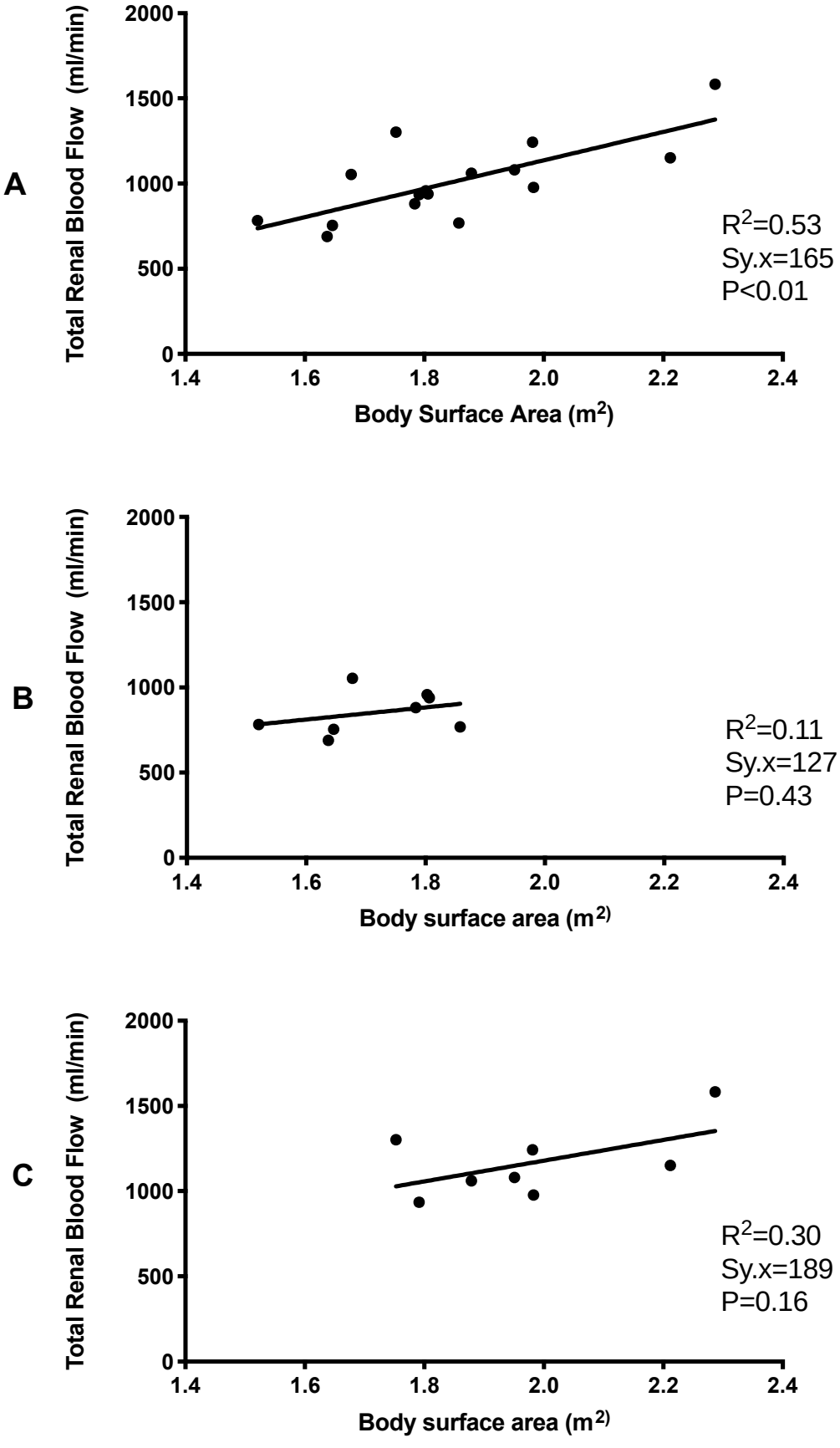
A
Total Renal Blood Flow (ml/min)
2000
1500
1000
500
0
1.4
1.6
1.8
2.0
2.2
2.4
Body Surface Area (m2)
R2=0.53
Sy.x=165
P<0.01
B
Total Renal Blood Flow (ml/min)
Body surface area (m2)
R2=0.11
Sy.x=127
P=0.43
C
Total Renal Blood Flow (ml/min)
Body surface area (m2)
R2=0.30
Sy.x=189
P=0.16

Figure 4.

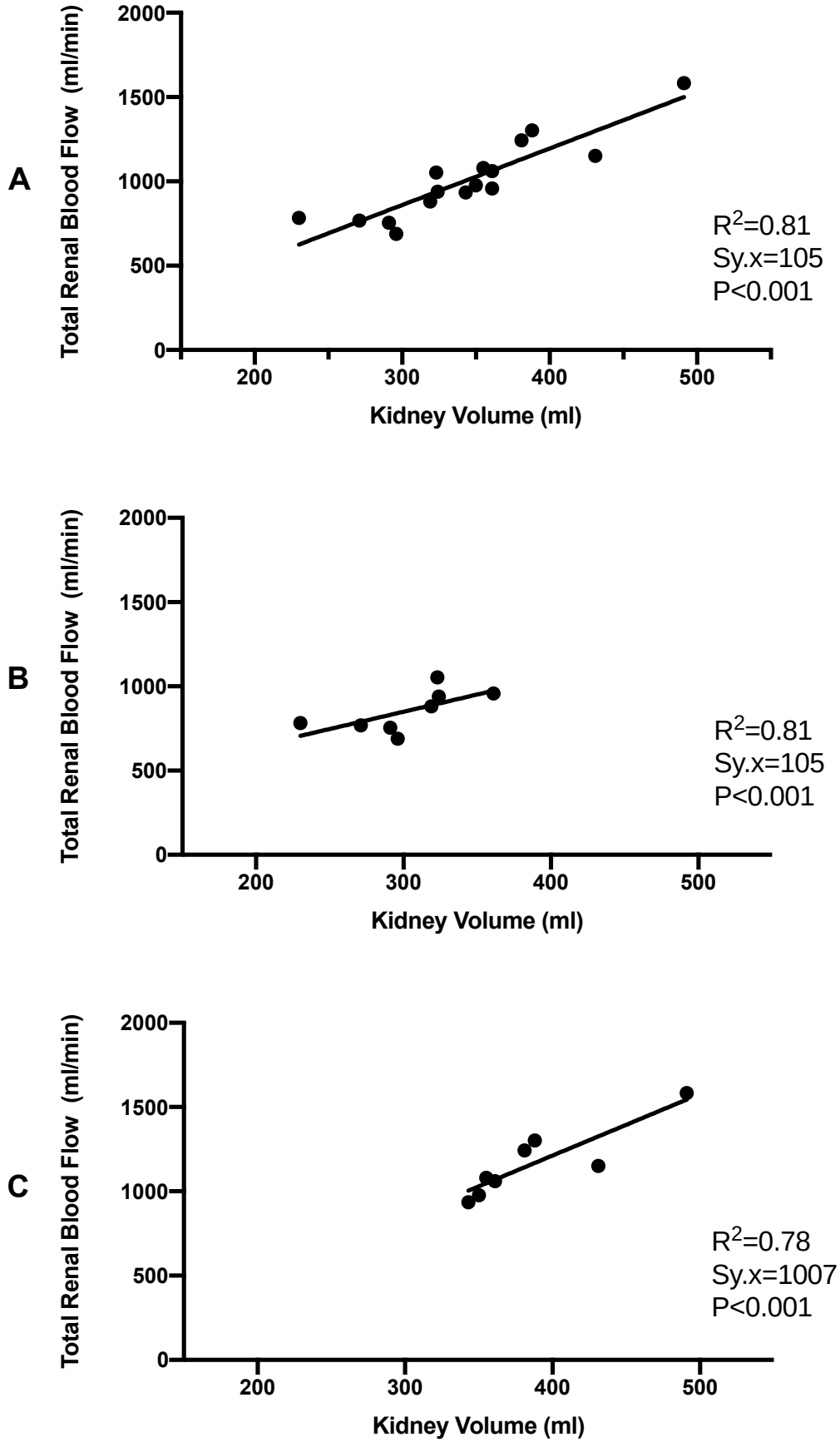
A
Total Renal Blood Flow (ml/min)
2000
1500
1000
500
0
200
300
400
500
Kidney Volume (ml)
R2=0.81
Sy.x=105
P<0.001
B
Total Renal Blood Flow (ml/min)
2000
1500
1000
500
0
200
300
400
500
Kidney Volume (ml)
R2=0.81
Sy.x=105
P<0.001
C
Total Renal Blood Flow (ml/min)
2000
1500
1000
500
0
200
300
400
500
Kidney Volume (ml)
R2=0.78
Sy.x=1007
P<0.001

Figure 5.

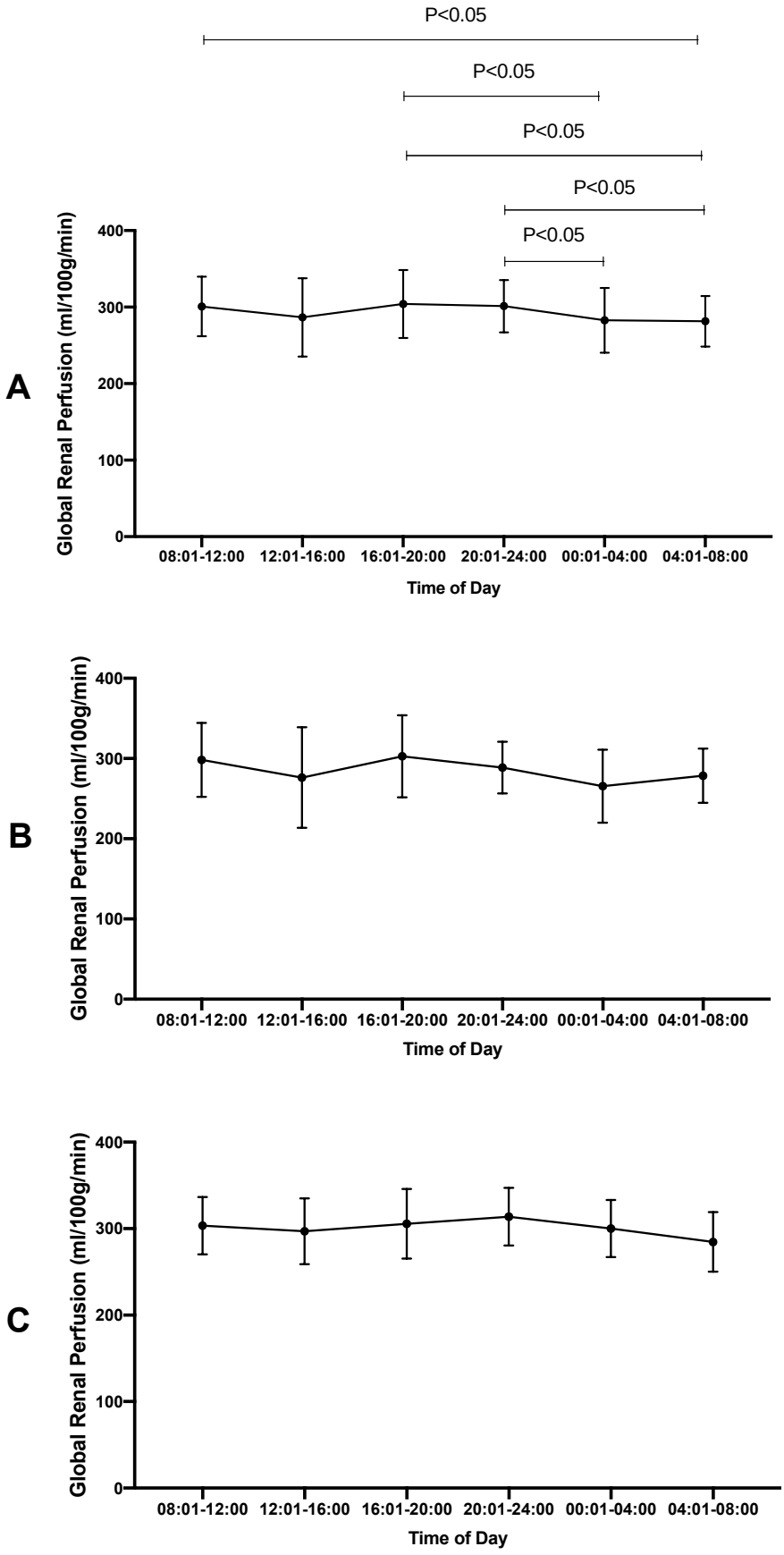
P<0.05
P<0.05
P<0.05
P<0.05
P<0.05
A
B
C
Global Renal Perfusion (ml/100g/min)
400
300
200
100
0
08:01-12:00
12:01-16:00
16:01-20:00
20:01-24:00
00:01-04:00
04:01-08:00
Time of Day

Figure 6.

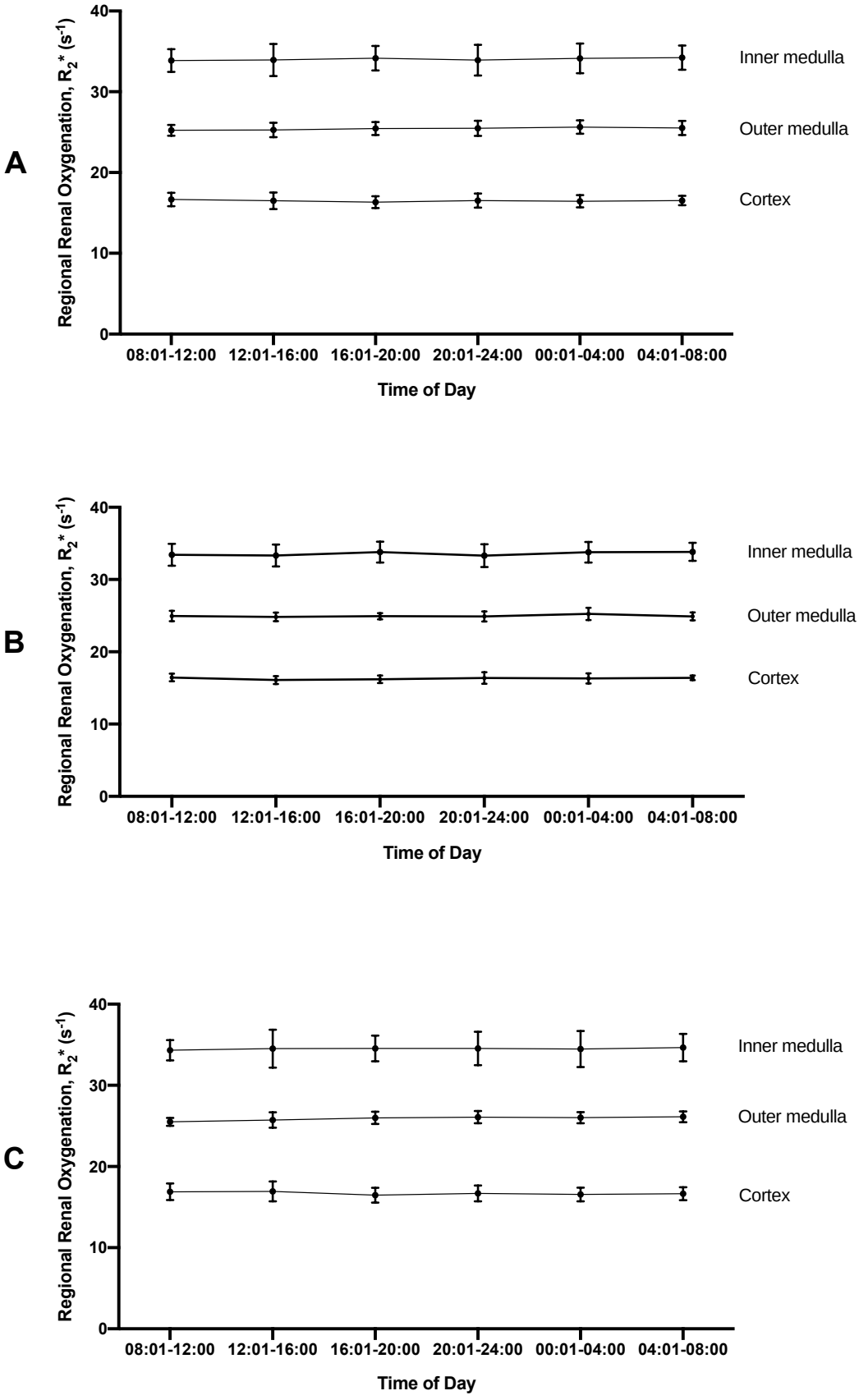
A
B
C
Regional Renal Oxygenation, R_2^* (s^{-1})
0
10
20
30
40
08:01-12:00
12:01-16:00
16:01-20:00
20:01-24:00
00:01-04:00
04:01-08:00
Time of Day
Inner medulla
Outer medulla
Cortex

Figure 7.

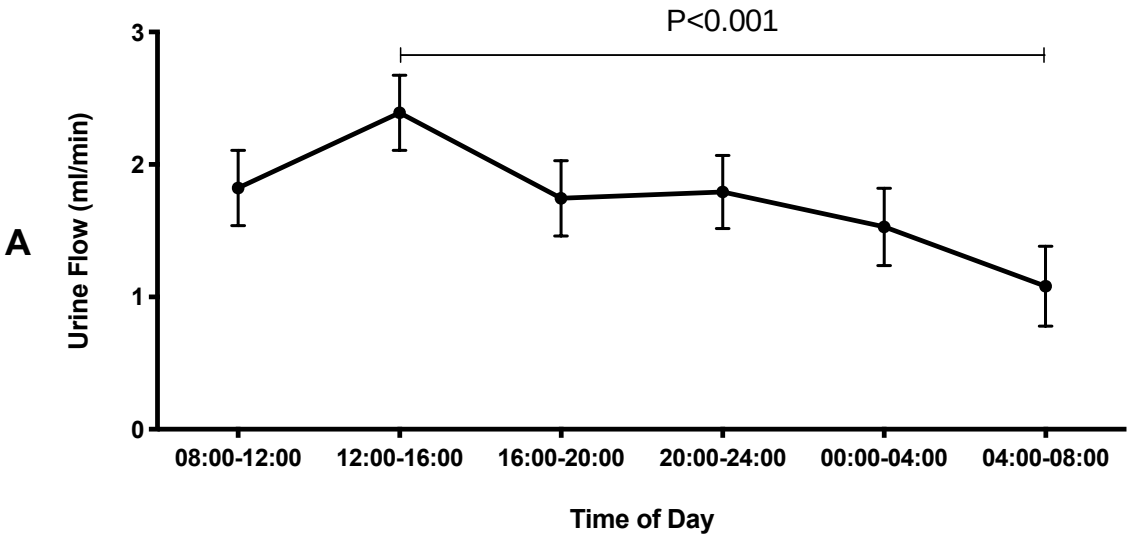
A
P<0.001
Urine Flow (ml/min)
3
2
1
0
08:00-12:00
12:00-16:00
16:00-20:00
20:00-24:00
00:00-04:00
04:00-08:00
Time of Day

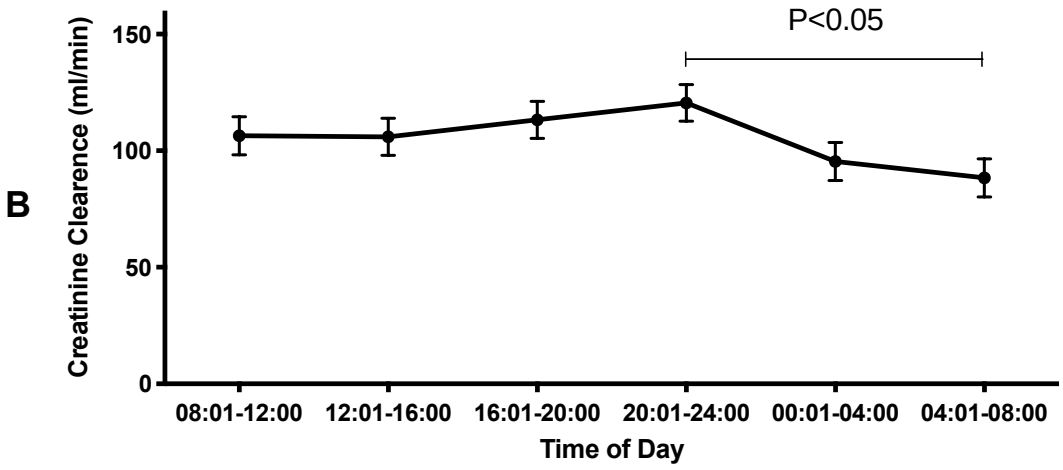
B
P<0.05
Creatinine Clearence (ml/min)
150
100
50
0
08:01-12:00
12:01-16:00
16:01-20:00
20:01-24:00
00:01-04:00
04:01-08:00
Time of Day

Figure 8.

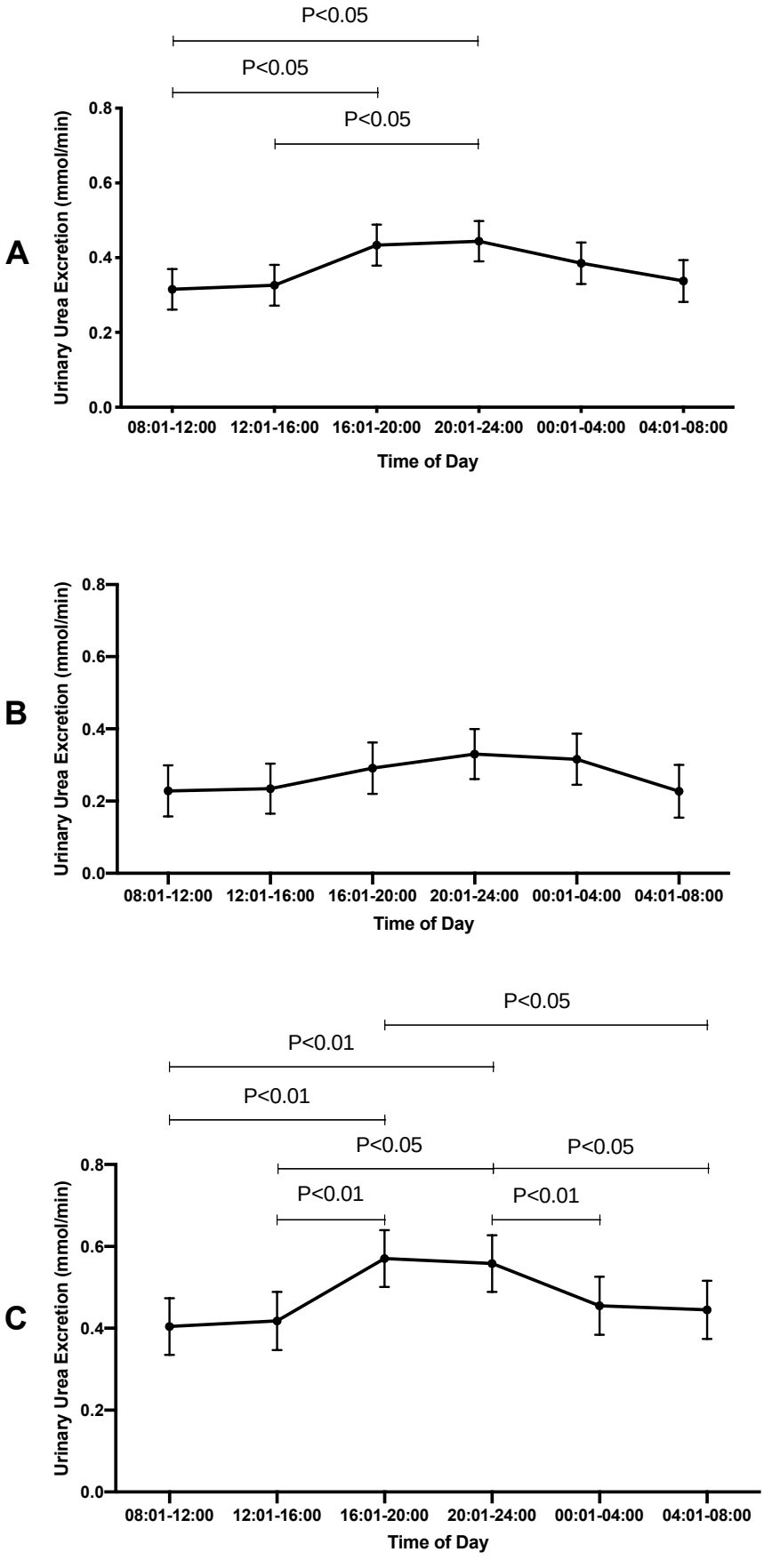
A
P<0.05
P<0.05
P<0.05
Urinary Urea Excretion (mmol/min)
0.0
0.2
0.4
0.6
0.8
08:01-12:00
12:01-16:00
16:01-20:00
20:01-24:00
00:01-04:00
04:01-08:00
Time of Day
B
Urinary Urea Excretion (mmol/min)
0.0
0.2
0.4
0.6
0.8
08:01-12:00
12:01-16:00
16:01-20:00
20:01-24:00
00:01-04:00
04:01-08:00
Time of Day
C
P<0.05
P<0.01
P<0.01
P<0.05
P<0.05
P<0.01
P<0.01
Urinary Urea Excretion (mmol/min)
0.0
0.2
0.4
0.6
0.8
08:01-12:00
12:01-16:00
16:01-20:00
20:01-24:00
00:01-04:00
04:01-08:00
Time of Day

Figure 9.

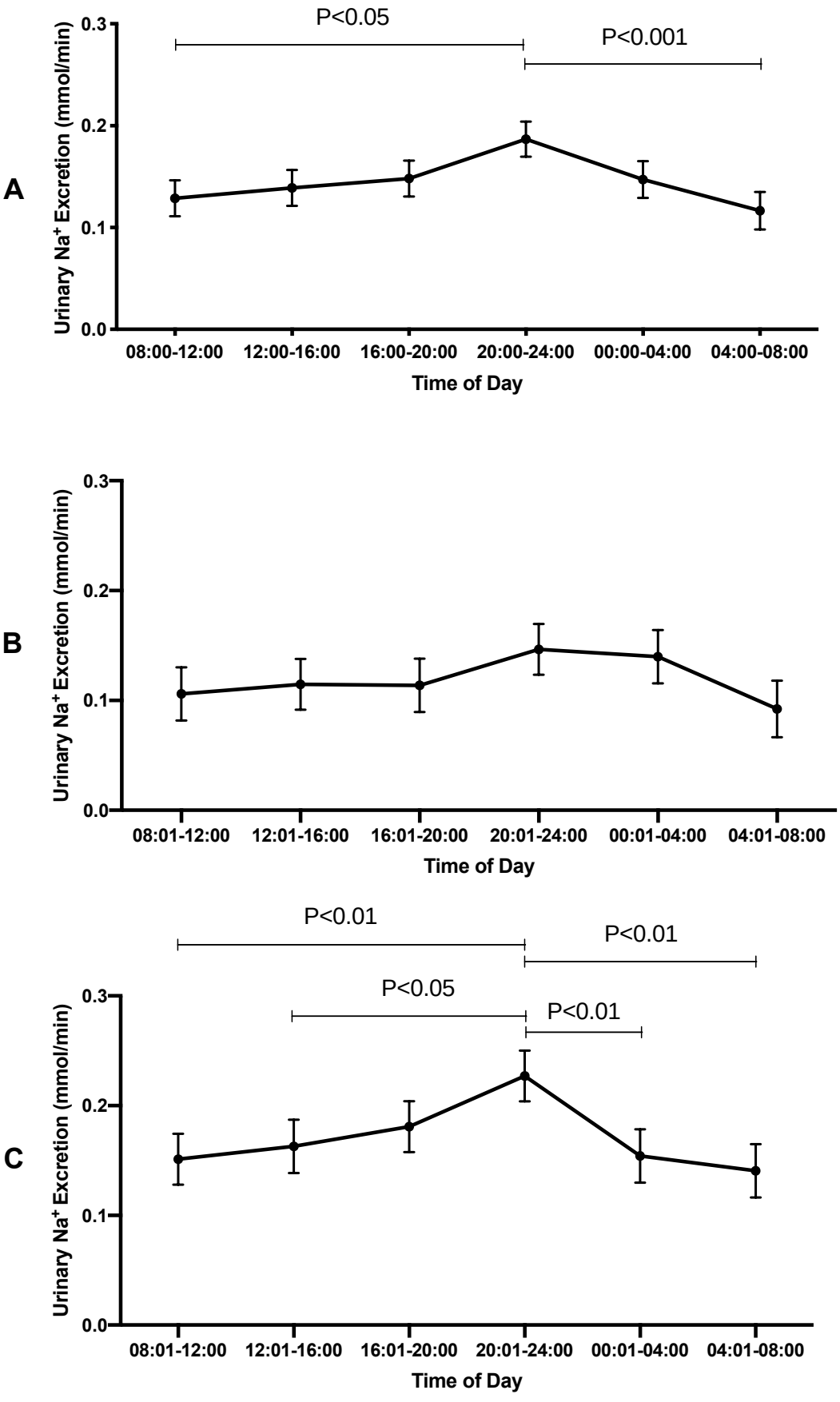
A
P<0.05
P<0.001
Urinary Na+ Excretion (mmol/min)
0.3
0.2
0.1
0.0
08:00-12:00
12:00-16:00
16:00-20:00
20:00-24:00
00:00-04:00
04:00-08:00
Time of Day
B
Urinary Na+ Excretion (mmol/min)
0.3
0.2
0.1
0.0
08:01-12:00
12:01-16:00
16:01-20:00
20:01-24:00
00:01-04:00
04:01-08:00
Time of Day
C
P<0.01
P<0.01
P<0.05
P<0.01
Urinary Na+ Excretion (mmol/min)
0.3
0.2
0.1
0.0
08:01-12:00
12:01-16:00
16:01-20:00
20:01-24:00
00:01-04:00
04:01-08:00
Time of Day

Figure 10.

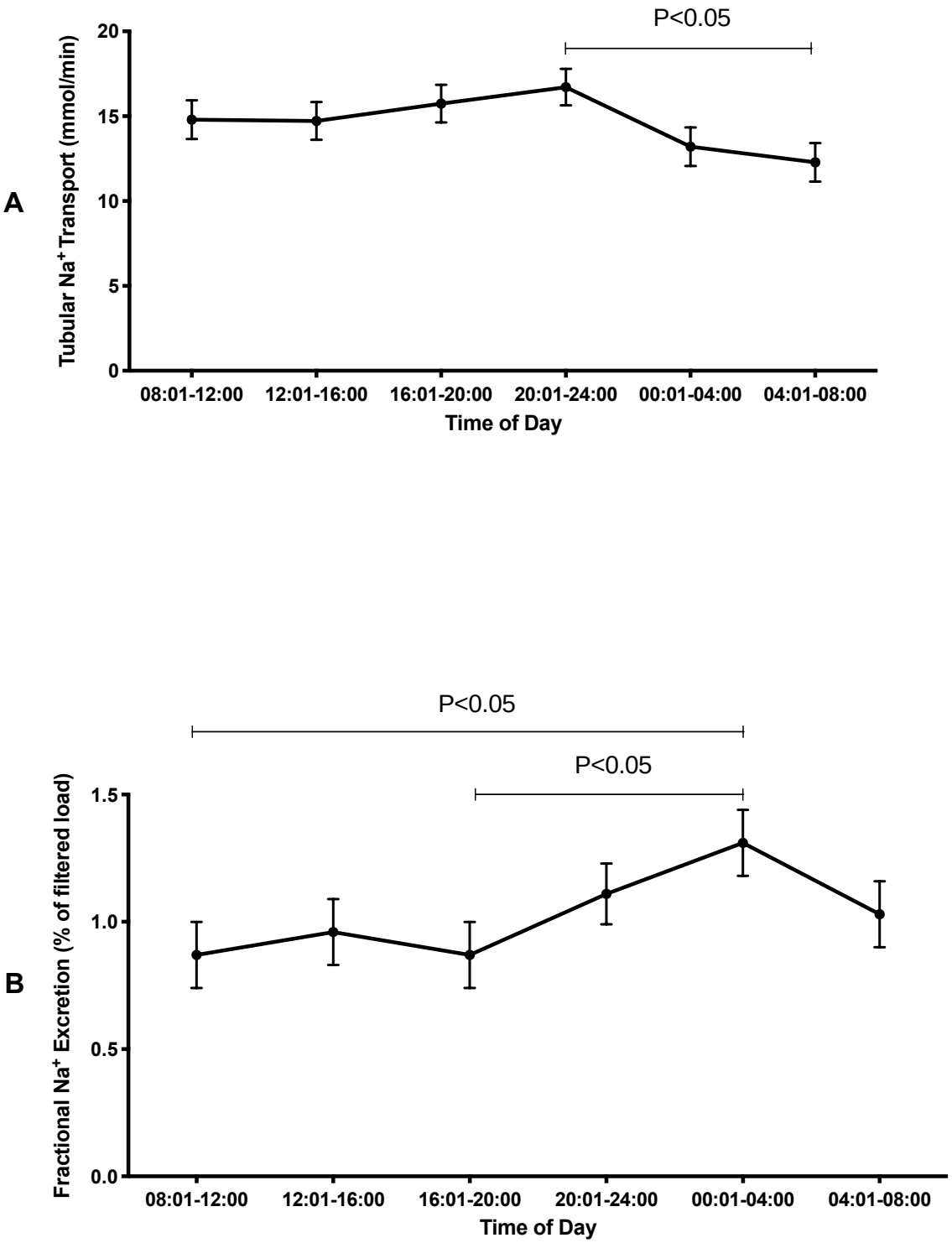
A
P<0.05
Tubular Na+ Transport (mmol/min)
20
15
10
5
0
08:01-12:00
12:01-16:00
16:01-20:00
20:01-24:00
00:01-04:00
04:01-08:00
Time of Day
B
P<0.05
P<0.05
Fractional Na+ Excretion (% of filtered load)
1.5
1.0
0.5
0.0
08:01-12:00
12:01-16:00
16:01-20:00
20:01-24:00
00:01-04:00
04:01-08:00
Time of Day

Figure 11.

References

1. Firsov D, Bonny O. Circadian rhythms and the kidney. Nat Rev Nephrol. 2018;14(10):626-35.
2. Smith E. On the elimination of urea and urinary water in relation to the period of the day, season, exertion, food, prison discipline, weight of body and other influences acting in the cycle of the year. . Phil Trans R Soc Lond. 1861;151:747–834
3. Smith E. Health and disease as influenced by the daily, seasonal, and other cyclical changes in the human system.
. Walton and Maberly, London
. 1861.
4. Potter GD, Skene DJ, Arendt J, Cade JE, Grant PJ, Hardie LJ. Circadian Rhythm and Sleep Disruption: Causes, Metabolic Consequences, and Countermeasures. Endocr Rev. 2016;37(6):584-608.
5. Firsov D, Bonny O. Circadian regulation of renal function. Kidney Int. 2010;78(7):640-5.
6. Gillette MU, Tischkau SA. Suprachiasmatic nucleus: the brain's circadian clock. Recent Prog Horm Res. 1999;54:33-58; discussion -9.
7. Cajochen C, Krauchi K, Wirz-Justice A. Role of melatonin in the regulation of human circadian rhythms and sleep. J Neuroendocrinol. 2003;15(4):432-7.
8. Brzezinski A. Melatonin in humans. N Engl J Med. 1997;336(3):186-95.
9. Tordjman S, Chokron S, Delorme R, Charrier A, Bellissant E, Jaafari N, et al. Melatonin: Pharmacology, Functions and Therapeutic Benefits. Curr Neuropharmacol. 2017;15(3):434-43.
10. Capsoni S, Stankov BM, Fraschini F. Reduction of regional cerebral blood flow by melatonin in young rats. Neuroreport. 1995;6(9):1346-8.
11. Weekley LB. Effects of melatonin on pulmonary and coronary vessels are exerted through perivascular nerves. Clin Auton Res. 1993;3(1):45-7.
12. Cook JS, Sauder CL, Ray CA. Melatonin differentially affects vascular blood flow in humans. Am J Physiol Heart Circ Physiol. 2011;300(2):H670-4.
13. Koopman MG, Koomen GC, Krediet RT, de Moor EA, Hoek FJ, Arisz L. Circadian rhythm of glomerular filtration rate in normal individuals. Clin Sci (Lond). 1989;77(1):105-11.
14. Mills JN, Stanbury SW. Persistent 24-hour renal excretory rhythm on a 12-hour cycle of activity. J Physiol. 1952;117(1):22-37.
15. Solocinski K, Gumz ML. The Circadian Clock in the Regulation of Renal Rhythms. J Biol Rhythms. 2015;30(6):470-86.
16. Emans TW, Janssen BJ, Joles JA, Krediet CTP. Circadian Rhythm in Kidney Tissue Oxygenation in the Rat. Front Physiol. 2017;8:205.
17. Adamovich Y, Ladeuix B, Golik M, Koeners MP, Asher G. Rhythmic Oxygen Levels Reset Circadian Clocks through HIF1alpha. Cell Metab. 2017;25(1):93-101.
18. Eckerbom P, Hansell P, Cox E, Buchanan C, Weis J, Palm F, et al. Multiparametric assessment of renal physiology in healthy volunteers using noninvasive magnetic resonance imaging. Am J Physiol Renal Physiol. 2019;316(4):F693-F702.
19. Bax L, Bakker CJ, Klein WM, Blanken N, Beutler JJ, Mali WP. Renal blood flow measurements with use of phase-contrast magnetic resonance imaging: normal values and reproducibility. J Vasc Interv Radiol. 2005;16(6):807-14.
20. Piskunowicz M, Hofmann L, Zuercher E, Bassi I, Milani B, Stuber M, et al. A new technique with high reproducibility to estimate renal oxygenation using BOLD-MRI in chronic kidney disease. Magn Reson Imaging. 2015;33(3):253-61.

21. Kim SG, Tsekos NV. Perfusion imaging by a flow-sensitive alternating inversion recovery (FAIR) technique: application to functional brain imaging. Magn Reson Med. 1997;37(3):425-35.
22. Palm F, Cederberg J, Hansell P, Liss P, Carlsson PO. Reactive oxygen species cause diabetes-induced decrease in renal oxygen tension. Diabetologia. 2003;46(8):1153-60.
23. Kwong KK, Chesler DA, Weisskoff RM, Donahue KM, Davis TL, Ostergaard L, et al. MR perfusion studies with T1-weighted echo planar imaging. Magn Reson Med. 1995;34(6):878-87.
24. Francis ST, Bowtell R, Gowland PA. Modeling and optimization of Look-Locker spin labeling for measuring perfusion and transit time changes in activation studies taking into account arterial blood volume. Magn Reson Med. 2008;59(2):316-25.
25. Mosteller RD. Simplified calculation of body-surface area. N Engl J Med. 1987;317(17):1098.
26. Littell RC, Milliken GA, Stroup WW, Wolfinger RD, Schabenberger R, Statistical Analysis System I. SAS for mixed models2015.
27. Dambreville S, Chapman AB, Torres VE, King BF, Wallin AK, Frakes DH, et al. Renal arterial blood flow measurement by breath-held MRI: Accuracy in phantom scans and reproducibility in healthy subjects. Magn Reson Med. 2010;63(4):940-50.
28. Boss A, Martirosian P, Graf H, Claussen CD, Schlemmer HP, Schick F. High resolution MR perfusion imaging of the kidneys at 3 Tesla without administration of contrast media. Rofo. 2005;177(12):1625-30.
29. Wuerzner G, Firsov D, Bonny O. Circadian glomerular function: from physiology to molecular and therapeutical aspects. Nephrol Dial Transplant. 2014;29(8):1475-80.
30. Somers VK, Dyken ME, Mark AL, Abboud FM. Sympathetic-nerve activity during sleep in normal subjects. N Engl J Med. 1993;328(5):303-7.
31. Miller JC, Horvath SM. Cardiac output during human sleep. Aviat Space Environ Med. 1976;47(10):1046-51.
32. Calhoun DA, Harding SM. Sleep and hypertension. Chest. 2010;138(2):434-43.
33. Ohkubo T, Hozawa A, Nagai K, Kikuya M, Tsuji I, Ito S, et al. Prediction of stroke by ambulatory blood pressure monitoring versus screening blood pressure measurements in a general population: the Ohasama study. J Hypertens. 2000;18(7):847-54.
34. Dolan E, Stanton AV, Thom S, Caulfield M, Atkins N, McInnes G, et al. Ambulatory blood pressure monitoring predicts cardiovascular events in treated hypertensive patients--an Anglo-Scandinavian cardiac outcomes trial substudy. J Hypertens. 2009;27(4):876-85.
35. Ben-Dov IZ, Kark JD, Ben-Ishay D, Mekler J, Ben-Arie L, Bursztyn M. Predictors of all-cause mortality in clinical ambulatory monitoring: unique aspects of blood pressure during sleep. Hypertension. 2007;49(6):1235-41.
36. DiBona GF, Kopp UC. Neural control of renal function. Physiol Rev. 1997;77(1):75-197.
37. Harrison-Bernard LM. The renal renin-angiotensin system. Adv Physiol Educ. 2009;33(4):270-4.
38. DiBona GF. Dynamic analysis of patterns of renal sympathetic nerve activity: implications for renal function. Exp Physiol. 2005;90(2):159-61.
39. Riquier-Brison AD, Leong PK, Pihakaski-Maunsbach K, McDonough AA. Angiotensin II stimulates trafficking of NHE3, NaPi2, and associated proteins into the proximal tubule microvilli. Am J Physiol Renal Physiol. 2010;298(1):F177-86.
40. Hurwitz S, Cohen RJ, Williams GH. Diurnal variation of aldosterone and plasma renin activity: timing relation to melatonin and cortisol and consistency after prolonged bed rest. J Appl Physiol (1985). 2004;96(4):1406-14.

41. Gordon RD, Wolfe LK, Island DP, Liddle GW. A diurnal rhythm in plasma renin activity in man. J Clin Invest. 1966;45(10):1587-92.
42. Brandenberger G, Follenius M, Goichot B, Saini J, Spiegel K, Ehrhart J, et al. Twenty-four-hour profiles of plasma renin activity in relation to the sleep-wake cycle. J Hypertens. 1994;12(3):277-83.
43. Chavarri M, Ganguly A, Luetscher JA, Zager PG. Effect of bedrest on circadian rhythms of plasma renin, aldosterone, and cortisol. Aviat Space Environ Med. 1977;48(7):633-6.
44. Modlinger RS, Sharif-Zadeh K, Ertel NH, Gutkin M. The circadian rhythm of renin. J Clin Endocrinol Metab. 1976;43(6):1276-82.
45. Gizowski C, Trudel E, Bourque CW. Central and peripheral roles of vasopressin in the circadian defense of body hydration. Best Pract Res Clin Endocrinol Metab. 2017;31(6):535-46.
46. Kalsbeek A, Palm IF, La Fleur SE, Scheer FA, Perreau-Lenz S, Ruiter M, et al. SCN outputs and the hypothalamic balance of life. J Biol Rhythms. 2006;21(6):458-69.
47. Kalsbeek A, Fliers E, Hofman MA, Swaab DF, Buijs RM. Vasopressin and the output of the hypothalamic biological clock. J Neuroendocrinol. 2010;22(5):362-72.
48. Tsuji T, Allchorne AJ, Zhang M, Tsuji C, Tobin VA, Pineda R, et al. Vasopressin casts light on the suprachiasmatic nucleus. J Physiol. 2017;595(11):3497-514.
49. Hume C, Allchorne A, Grinevich V, Leng G, Ludwig M. Effects of optogenetic stimulation of vasopressinergic retinal afferents on suprachiasmatic neurons. J Neuroendocrinol. 2019.
50. Campos LA, Cipolla-Neto J, Amaral FG, Michelini LC, Bader M, Baltatu OC. The Angiotensin-melatonin axis. Int J Hypertens. 2013;2013:521783.
51. Ohashi N, Ishigaki S, Isobe S. The pivotal role of melatonin in ameliorating chronic kidney disease by suppression of the renin-angiotensin system in the kidney. Hypertens Res. 2019;42(6):761-8.
52. Koch BC, van der Putten K, Van Someren EJ, Wielders JP, Ter Wee PM, Nagtegaal JE, et al. Impairment of endogenous melatonin rhythm is related to the degree of chronic kidney disease (CREAM study). Nephrol Dial Transplant. 2010;25(2):513-9.
53. Matsubara M. Renal sodium handling for body fluid maintenance and blood pressure regulation. Yakugaku Zasshi. 2004;124(6):301-9.
54. Nikolaeva S, Pradervand S, Centeno G, Zavadova V, Tokonami N, Maillard M, et al. The circadian clock modulates renal sodium handling. J Am Soc Nephrol. 2012;23(6):1019-26.
55. Wei N, Gumz ML, Layton AT. Predicted effect of circadian clock modulation of NHE3 of a proximal tubule cell on sodium transport. Am J Physiol Renal Physiol. 2018;315(3):F665-F76.
56. McDonald KM, Miller PD, Anderson RJ, Berl T, Schrier RW. Hormonal control of renal water excretion. Kidney Int. 1976;10(1):38-45.
57. Goh MY, Millard MS, Wong EC, Brown DJ, Frauman AG, O'Callaghan CJ. Diurnal blood pressure and urine production in acute spinal cord injury compared with controls. Spinal Cord. 2017;55(1):39-46.
58. Blanker MH, Bernsen RM, Ruud Bosch JL, Thomas S, Groeneveld FP, Prins A, et al. Normal values and determinants of circadian urine production in older men: a population based study. J Urol. 2002;168(4 Pt 1):1453-7.
59. Nakamura S, Kobayashi Y, Tozuka K, Tokue A, Kimura A, Hamada C. Circadian changes in urine volume and frequency in elderly men. J Urol. 1996;156(4):1275-9.
60. Maher JF. Pathophysiology of renal hemodynamics. Nephron. 1981;27(4-5):215-21.
61. Evans RG, Smith DW, Lee CJ, Ngo JP, Gardiner BS. What Makes the Kidney Susceptible to Hypoxia? Anat Rec (Hoboken). 2019.

62. Liss P, Nygren A, Revsbech NP, Ulfendahl HR. Intrarenal oxygen tension measured by a modified clark electrode at normal and low blood pressure and after injection of x-ray contrast media. Pflugers Arch. 1997;434(6):705-11.
63. Brezis M, Rosen S. Hypoxia of the renal medulla--its implications for disease. N Engl J Med. 1995;332(10):647-55.
64. Epstein FH, Agmon Y, Brezis M. Physiology of renal hypoxia. Ann N Y Acad Sci. 1994;718:72-81; discussion -2.
65. Brezis M, Agmon Y, Epstein F. Determinants of intrarenal oxygenation I. Effects of diuretics. Am J Physiol. 1994;267:F1059-F62.
66. Palm F, Nordquist L. Renal oxidative stress, oxygenation, and hypertension. Am J Physiol Regul Integr Comp Physiol. 2011;301(5):R1229-41.
67. O'Connor PM. Renal oxygen delivery: matching delivery to metabolic demand. Clin Exp Pharmacol Physiol. 2006;33(10):961-7.
68. Honda T, Hirakawa Y, Nangaku M. The role of oxidative stress and hypoxia in renal disease. Kidney Res Clin Pract. 2019;38(4):414-26.
69. Denys MA, Viaene A, Goessaert AS, Van Haverbeke F, Hoebeke P, Raes A, et al. Circadian Rhythms in Water and Solute Handling in Adults with a Spinal Cord Injury. J Urol. 2017;197(2):445-51.
70. Tojo A, Kinugasa S. Mechanisms of glomerular albumin filtration and tubular reabsorption. Int J Nephrol. 2012;2012:481520.
71. Buzio C, Mutti A, Capani F, Andrulli S, Perazzoli F, Alinovi R, et al. Circadian rhythm of proteinuria: effects of an evening meat meal. Nephrol Dial Transplant. 1989;4(4):266-70.
72. Kanabrocki EL, Kanabrocki JA, Sothern RB, Futscher B, Lampo S, Cournoyer C, et al. Circadian distribution of proteins in urine from healthy young men. Chronobiol Int. 1990;7(5-6):433-43.
73. Rabinowitz L. Aldosterone and potassium homeostasis. Kidney Int. 1996;49(6):1738-42.
74. Picazo A, Jimenez-Osorio AS, Zuniga-Mejia P, Pedraza-Chaverri J, Monroy A, Rodriguez-Arellano ME, et al. Hypoglycemic drugs induce antioxidant aldehyde dehydrogenase activity and remain high in patients with glycemic control in type 2 diabetes. Eur J Pharmacol. 2017;800:57-62.
75. Yavuzer H, Yavuzer S, Cengiz M, Erman H, Doventas A, Balci H, et al. Biomarkers of lipid peroxidation related to hypertension in aging. Hypertens Res. 2016;39(5):342-8.